Study of Fiber Bragg Grating Samples Exposed to High Fast Neutron Fluences

G. Cheymol, L. Remy, A. Gusarov, D. Kinet, P. Mégret, Guillaume Laffont, Thomas Blanchet, A. Morana, E. Marin, S. Girard

Study of Fibre Bragg Grating samples exposed to High Fast-Neutron Fluences

G. Cheymol, L. Remy, A. Gusarov, D. Kinet, P. Megret, G. Laffont, T. Blanchet, A. Morana, E. Marin, S. Girard

HAL Id: cea-02339816

https://hal-cea.archives-ouvertes.fr/cea-02339816

Submitted on 5 Nov 2019

Study of Fibre Bragg Grating samples exposed to High Fast-Neutron Fluences

G. Cheymol, L. Remy, A. Gusarov, D. Kinet, P. Mégret, G. Laffont, T. Blanchet, A. Morana, E. Marin
and S. Girard *Senior Member, IEEE*

Abstract–**Fibre Bragg Grating (FBG) sensors are expected to provide valuable data in extreme radiation environments associated with nuclear research reactors. However, when the fast neutron fluence reaches 10^{18} to 10^{19} n/cm², the radiation induced changes in the material density and refractive index may drastically bias the measurements. The present study evaluates the radiation effect on the FBG performances by comparing their properties before and after their exposure to fast neutron fluences exceeding 10^{19} n/cm² (E > 1 MeV). We studied responses of FBGs manufactured by three different laboratories in the same single-mode optical fibre but using different inscription conditions. The Bragg wavelength and the reflectivity were measured before and after irradiation thanks to a dedicated mounting. For nearly all FBGs, the Bragg peak remains visible after the irradiation while the radiation-induced Bragg wavelength shifts (RI-BWS) vary from a few pm (equivalent temperature error < 1°C) to nearly 1 nm (~100°C error) depending of the FBG inscription conditions. Such high RI-BWSs can be explained by the huge refractive-index variation and compaction observed for bare fibre samples through other experimental techniques. Our results show that by using specific hardening techniques the FBG-based temperature measurements in a nuclear research reactor experiment may become feasible.**
Index terms– **Fibre Bragg grating, optical fibre sensors, radiation effect, optical fibres, neutron, gamma, compaction.**

I. Introduction

AMONG R&D programs, effective irradiation experiments in Material Testing Reactors (MTR) are required to support lifetime extension, better fuel management

and increased safety of existing and future nuclear power plants. For example, the Jules Horowitz Reactor (JHR), a new MTR under construction in Cadarache (France) is expected to feature experiments with new, improved instrumentation [1]. The use of enhanced in-core online monitoring is also considered for next generations of power reactor, particularly for the ASTRID (Advanced Sodium Technological Reactor for Industrial Demonstration) prototype [2], developed in France and for MYRRHA (Multi-purpose hYbrid Research Reactor for High-tech Applications) project [3] developed in Belgium.

For such objective, Optical Fibre Sensors (OFS) display some attractive features: compact size, remote multi-point or distributed sensing, passive operation, low sensitivity to electromagnetic interference, as well as high spatial and time resolutions and low uncertainty [4]. But their performances can be affected under high levels of radiation. The Radiation Induced Attenuation (RIA) in silica-based optical fibres is probably the most known effect [5]. The effect of RIA and the subsequent dynamic range loss can be limited to some extent by using radiation hardened fibres. But radiation induced emission and compaction caused by high fluxes and fast neutron fluences must also be taken into account, see for example [6] for the influence on the Fabry Perot sensor (FPS). When the fast neutron fluence reaches 10^{18} to 10^{19} n/cm², the density and refractive index variations related to structural changes of the pure or doped silica drastically deteriorate the OFS performances even for those based on rad hard fibres.

In the framework of the Joint Instrumentation Laboratory, gathering SCK·CEN (The Belgium Nuclear Research Center) and CEA (French Nuclear Atomic Agency), the presented study aims to assess the effect of nuclear radiations on the FPS and on the Fibre Bragg Grating (FBG) sensors by comparing the performances of these OFSs before and after irradiation. The main targeted FBG application in MTRs and other reactors concerns multipoint temperature sensing with a spatial resolution as low as 10 mm. The use of a FBG based strain sensor may also be considered in the future.

Analysis of the FPS reactor irradiation data demonstrated that the sensor can suffer from a significant drift [6]. To understand reasons for such response two additional irradiation campaigns were performed, named SAKE 1 (Smirnof extension - Additional Key-tests on Elongation of glass fibres) and SAKE 2. The experiments involved few centimetres long fibre samples, functionalized or not. The results of SAKE 1 were reported in [7]. Beside the fact that

G. Cheymol, L. Remy, are with Den – Service d'Etudes Analytiques et de Réactivité des Surfaces (SEARS), CEA, Université Paris-Saclay, F-91191, Gif sur Yvette, France (33(0)1.69.08.62.71; e-mail: guy.cheymol@cea.fr, e-mail: laurent.remy@cea.fr).

A. Gusarov is with SCK•CEN - Belgian Nuclear Research center, Boeretang 200 2400 Mol Belgium (e-mail: andrei.goussarov@sckcen.be).

D. Kinet and P. Mégret are with the Electromagnetism and Telecommunications Department of the University of Mons, 31 Boulevard Dolez, 7000 Mons, Belgium (e-mail: damien.kinet@umons.ac.be).

G. Laffont and T. Blanchet are with the Technological Research Division (TRD) of the French Alternative Energies and Atomic Energy Commission. F-91191, Gif sur Yvette, France (e-mail : guillaume.laffont@cea.fr; thomas.blanchet@cea.fr)

T. Blanchet, A. Morana, E. Marin, and S. Girard are with Université de Saint-Etienne, Laboratoire Hubert Curien, UMR CNRS 5516, 18, rue du Pr. Lauras, F-42000 Saint-Etienne, France (e-mails : adriana.morana@univ-st-etienne.fr ; emmanuel.marin@univ-st-etienne.fr; sylvain.girard@univ-st-etienne.fr).

uncoated fibre samples irradiated in the MTR core could be successfully handled to perform post-irradiation measurements and give appreciated results, the main conclusion was that the mean value of the obtained compaction after exposition to 3 to 5×10^{19} n_{fast}/cm², at 290 °C, for the pure silica core fibre used in the FPSs, was less than what could be expected from the measurements on bulk silica samples made by Primak [8] in the sixties: 0.27% instead of 1%. Also, measurements performed on a few FBG samples gave promising results for the use of FBG sensors in such a severe radiation environment.

SAKE 2 campaign was intended to confirm compaction measurements on a larger set of fibre samples and to perform a complete survey of FBG responses enlarging the variety of tested samples, mainly FBGs hardened against irradiation and high temperatures.

A FBG consists of a periodic modulation of the refractive index of the fibre core with a typical period of 1 µm or shorter[1]. In a single-mode fibre this modulation results in a wavelength selective coupling of the forward-propagating mode to the backward propagating one, i.e. the component corresponds to a pass-band filter in reflection and a rejection band filter in transmission centred at the Bragg wavelength λ_B, which is defined as:

$$\lambda_B = 2n_{eff}\Lambda_B, \qquad (1)$$

where n_{eff} is the effective refractive index of the propagating core mode and Λ is the grating period.

Among other parameters, a change of the environment temperature changes the Bragg wavelength λ_B through variations in n_{eff} and Λ values, allowing to design a temperature sensor, which relies on the linear[2] relationship:

$$\lambda_B(T) = \lambda_B(T_0) + \alpha(T - T_0), \qquad (2)$$

where T_0 is a reference temperature and α is the temperature sensitivity coefficient with a typical value of ~10 pm/K at 1550 nm.

The quality of the FBG temperature sensor measurements can be influenced by radiation. Indeed, radiation-induced dilatations impact Λ, and both the RIA and compaction phenomena induce changes in n_{eff}. Those changes are described through the Kramers-Kronig relation and the Lorentz-Lorenz equation, respectively. Therefore a radiation-induced BWS appears and causes an error on the temperature measurement. Furthermore, irradiation can also affect the spectral shape of the Bragg peak, in certain cases leading to its complete erasure. In case the shape of the Bragg peak changes with the dose, the procedure used to retrieve λ_B becomes crucial.

There exist extensive literature dedicated to radiation effects in FBGs, see for example recent review papers [9-10]. While numerous papers relate the effects of gamma radiations on FBG and methods in overcoming them [11-13], only a few [14-17] deal with the combined effects of gamma radiations and high fluences of fast neutrons.

Temperature during irradiation is an important parameter to consider. Firstly, because the targeted applications operate at temperatures of several hundreds of Celsius degrees, which can deeply reduce or even erase the Bragg peak, and secondly, because temperature influences the amplitudes and kinetics of radiation effects [18].

We focus the present paper on the FBGs written by different techniques in the SMF28 fibre by Corning, both more common type I FBGs and radiation hardened type II FBGs. A few other results are presented, particularly measurements obtained on FBGs written in pre-irradiated fibre samples. The tested FBGs were provided by three research labs involved. The Bragg wavelengths of all samples are located in the 1.55 µm window. Both measurements of the change in the Bragg peak amplitude and the BWS are reported.

The two levels of neutron fluence were selected by taking the previous compaction measurements into consideration. At 3×10^{19} n_{fast}/cm² compaction should have reached saturation according to Primak work [8], and our SAKE 1 results [7] that showed no significant difference between the compactions measured at 3 or 5 $\times 10^{19}$ n_{fast}/cm². A smaller fluence of 10^{19} n_{fast}/cm² was chosen as we expected that at this level the changes are not saturated yet and the FBGs response should be clearly different.

Small samples of uncoated fibres with one grating written in were irradiated in capsules. This configuration did not allow a continuous monitoring of the Bragg peak during the irradiation but it allowed irradiating many samples simultaneously.

The paper is organised as follows: the samples under test are described in the next section as well as the experimental procedure. The obtained results are given in section IV. Complementary measurements of compaction and subsequent refractive index variation are also presented in order to support the discussion.

II. INVESTIGATED FIBRE BRAGG GRATINGS

A. Tested Fibre Bragg Gratings

All the FBGs were written in SMF28 or SMF28e fibres, with the exception of two gratings written in a pre-irradiated pure silica fibre.

Table I gives a summary of the tested FBGs written in SMF28 or SMF28e fibres. A1, A2 and A3 are standard Type I saturated FBG manufactured by CEA List, Saclay, France using a continuous-wave 244 nm laser. B1 and B2 are radiation-hardened fibre Bragg gratings manufactured by Laboratoire Hubert Curien of Saint Etienne, France, using a dedicated technique that has already demonstrated its efficiency in improving the FBG radiation tolerance [11, 19]. The phase-mask technique was applied in combination with a Ti:Sapphire laser emitting 50 fs long pulses of 500 µJ energy at 800 nm with a repetition rate of 1 kHz. The laser beam was focused on the optical fibre core by the help of a cylindrical lens having a focal length of 10 mm; a transversal scan of the beam along the whole fibre core was performed at a frequency

---

[1] Long Period Gratings are not considered in this study.
[2] With limited temperature variations

of 25 mHz to optimize the induced refractive index structuration. After inscription, an annealing at 750°C for 2 hours was performed, as it has been demonstrated that such thermal treatment increases the FBG radiation-resistance. It should be noted that the annealing process used here differs from the usual regeneration process applied to Type-1 FBGs [20].

FBGs labelled C1 to C7 were fabricated at the Electromagnetism and Telecommunication Department of UMONS, Mons, Belgium. These ones were written into hydrogenated (200 bars at 68°C during 30 hours) and non-hydrogenated fibres by means of a femtosecond Ti:Sapphire SpitFire laser from Newport emitting at 800 nm, through a 1070 nm-period uniform phase mask. An adjustable diaphragm was placed to select a uniform energy region of the IR beam. The FBG's length of 7 mm was defined by the aperture of the diaphragm.

TABLE 1. CHARACTERISTICS OF FBGS WRITTEN ON SMF28 TYPE FIBRE

FBG	Inscription	H_2 Loading	Thermal treatment Temperature (°C)
A1-A3	UV-CW / 244 nm	yes	-
B1-B2	fs / 800 nm	no	750°C/2h
C1-C3	fs / 800 nm	yes	372°C/72h
C4-C7	fs / 800 nm	no	372°C/72h

Structural modifications associated with neutron induced compaction are supposed to affect drastically the Bragg peak. As the compaction tends to saturate at about 3×10^{19} n_{fast}/cm^2 [7-8], writing a FBG in a pre-irradiated fibre was considered of interest in order to obtain a rad-hard FBG. LabHC wrote two FBGs in uncoated pure-silica SM fibre samples previously irradiated at 5×10^{19} n_{fast}/cm^2 during SAKE 1 campaign [7]. The compaction was measured at 0.27% for these samples. We must note that the inscription in such irradiated samples was far more complex than in pristine fibres since the usual procedures allowing to monitor the Bragg peak growth during the inscription were no more accessible. The characteristics of those two FBGs are reported in Table 2.

TABLE 2. CHARACTERISTICS OF FBGS WRITTEN ON PRE-IRRADIATED SAMPLES

FBG	Inscription	Pre-irradiation	Thermal treatment Temperature (°C)
D1	fs / 800 nm	5×10^{19} $n_{fast}.cm^{-2}$	-
D2	fs / 800 nm	5×10^{19} $n_{fast}.cm^{-2}$	750°C/2h

B. Samples Preparation

All irradiated samples were uncoated fibres tips with the length ranging from 30 to 50 mm. The differences in the length allowed to distinguish the samples after irradiation since no other marking which could survive the reactor exposure was possible. Such fibre samples have small mass - less than 1.5 mg - which greatly alleviates the activation problem. It should be noted that the uncoated samples are fragile and required very careful handling. The two faces of each fibre sample were cleaved to allow both reflection and transmission measurements.

III. EXPERIMENTAL PROCEDURE

The samples were inserted in two different capsules (one for each fluence). The reactor exposure was performed using the BAMI (BAsket for Material Irradiation) irradiation rig of the BR2 reactor. The outer envelope of the capsules was maintained at about 50°C by the reactor cooling water. Thermal insulation achieved by a helium gas gap between the wall of the capsule and the inner aluminium body, coupled with the gamma heating of the inner body, kept the inner temperature at 250°C ± 25°C, according to calculations[3]. The inner body contained 5 channels of 2 mm in diameter each, in which the fibre samples were placed (figure 1).

Fig.1. Left: two capsules with inner body and outside wall; right: top view of the inner body (diameter 19mm, height 60 mm) with 5 compartments.

After insertion of the fibre samples, the capsules were hermetically sealed. Since two different fluences of neutrons were expected but at the same temperature, and as the heating was produced by radiations, the two capsules were irradiated approximately at the same height in the reactor core, so that they got the same gamma radiation flux. Capsule 1 was removed after 75 h of irradiation and Capsule 2 after 225 h.

Activation dosimeters were also placed in the capsules. The equivalent fission flux was calculated from the ^{54}Mn activity formed by the reaction $^{54}Fe(n,p)^{54}Mn$. This reaction has an effective threshold energy of about 1 MeV. To obtain the flux value for the fast neutrons (E > 1 MeV), the equivalent fission flux was corrected with a factor 1.03, obtained through Monte Carlo N-Particle Code (MNCP) calculations of the BR2 neutron energy spectrum. The irradiation conditions are summarized in Table 3:

TABLE 3. SUMMARY OF THE IRRADIATION CONDITIONS IN THE REACTOR BR2 FOR THE 2 CAPSULES

Capsule	Temperature (°C)	Flux ($n_{fast}.cm^{-2}.s^{-1}$)*	Duration h	Fluence ($n_{fast}.cm^{-2}$)
1	250 ± 25	3×10^{13}	75	10^{19}
2	250 ± 25	3×10^{13}	225	3×10^{19}

* E > 1 MeV

The corresponding gamma flux was about 2 W/g, i.e. 7.2 MGy/h, leading to the cumulated ionizing doses of 0.5 and 1.5 GGy for capsules 1 and 2 respectively.

[3] According to calculations. No monitoring of the inner temperature was possible.

The distribution of the tested samples between the two fluences is displayed in Table 4:

TABLE 4. DISTRIBUTION OF SAMPLES BETWEEN THE TWO FLUENCES:

FBG	10^{19} $n_{fast}.cm^{-2}$	3×10^{19} $n_{fast}.cm^{-2}$
A1-A3	x	
B1	x	
B2		x
C1-C5	x	
C6-C7		x
D1-D2		x

Once the irradiation fluence for each capsule was reached, the capsules were extracted from the reactor core and left for two months to decrease the activation levels. The cutting and unloading of the samples was achieved in a hot cell. The fibre samples of each hole were poured out in a separate container. The post-irradiation analysis started in several weeks. The delays were not expected to influence too much the measurements since the changes produced by the high fast neutron fluences are mainly structural and are not expected to anneal significantly at room temperature.

IV. FIBRE BRAGG GRATING CHARACTERIZATION SET UP

FBGs were characterized both before (BI) and after irradiation (PI standing for Post Irradiation). RI-BWS was the main expected output of the measurements. However, the change in the FBG reflectivity was also monitored as its decrease indicates that at a larger fluence, the FBG can either disappear or the uncertainty in measuring the BWS can increase.

A. Measurements

The FBGs' Bragg peak was measured both in reflection and transmission with an Anritsu MS9740A Optical Spectrum Analyzer (OSA) and a broad-band SLED source. The BWS was nominally deduced from the reflection measurements and the reflectivity from the transmission measurements. In some cases radiation deeply affected the FBG, and the Bragg peak was hardly distinguishable on the transmitted spectrum. Then, the reflected spectrum was used to characterize both the BWS and the reflectivity.

The measurement set-up is depicted in Figure 2. The SLED had a 80 nm 3dB bandwidth centred on 1550 nm. The same Anritsu MS9740A OSA was connected in two different positions according to the selected type of measurement. It has a spectral resolution of 0.03 nm on the spectral range of interest. Each spectrum was obtained by averaging 3 or more consecutive spectra. Let us note that the 50:50 optical fibre coupler is not needed in the transmission mode, but it was kept in order to avoid uncertainties related to reconnections. Since the temperature changes the Bragg wavelength, it was controlled during before and after irradiation measurements at 22°C ± 1°C. The temperature of the support was measured in

order to compensate small temperature differences when they had significant impact on the value of the BWS.
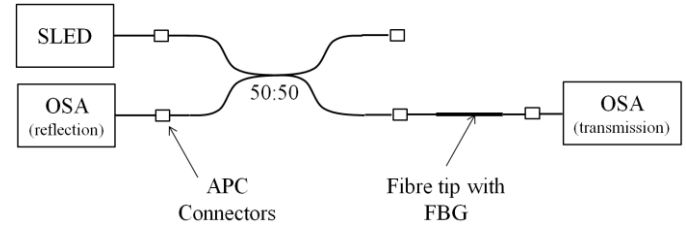

Fig. 2. Schematic diagram of the experimental set-up for the FBG interrogation in reflection or transmission; index matching liquid was added to the ends of the fibre tips. The same OSA was placed either in the "OSA reflection" position, for the reflection measurement or in the "OSA transmission" position, for the transmission measurement.

B. Assessment of the reflectivity – Attenuation

Change in reflectivity gives information on how the Bragg peak is affected by radiations. When the reflection peak is saturated (100% reflectivity), the change in its width is then used to highlight the radiation influence.

Generally the reflectivity was assessed through the transmission measurement. A typical example, sample C1, is given in Fig. 3. We calculated the transmission loss at the Bragg peak by subtracting the mean level beside the Bragg peak to its minimum:

$$T_{dB} = P_{T_{Bragg},dBm} - P_{T,dBm}; \quad R = 1 - T = 1 - 10^{0.1 \cdot T_{dB}} \quad (3)$$

In the example below, we obtain $T_{dB} = -6.7dB$ giving $T \sim$ 20% and then $R \sim 80\%$.
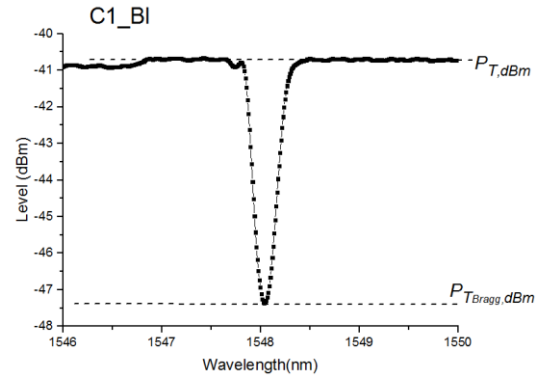

Fig. 3. Sample C1 transmission spectrum before irradiation, corresponding to an 80% reflectivity.

In case of a high reflectivity, when the deep amplitude in transmission exceeds 30 dB (reflectivity > 99.9%) the reflectivity is taken as 100%. Generally in that case acquisition shows a saturated reflection spectrum.

On the contrary, for low reflectivity cases, when the Bragg peak became hard to distinguish on the transmitted spectrum, the reflection spectrum was used to measure the reflectivity (but the level in transmission was still required):

$$R_{dB} = P_{R_{Bragg},dBm} - P_{T,dBm} + 3dB \quad (4)$$

The additional 3dB in the above relationship stands for the optical loss of the coupler as no additional loss impacts differently the transmitted and reflected signals. Particularly, the quality of butt-coupling to the fibre strand containing the grating strongly influenced the obtained value through the

transmission loss or Fresnel reflection at the interfaces that are likely to differently affect $P_{R_{Bragg},dBm}$ and $P_{T,dBm}$. This method is less precise even if the use of index matching gel avoided large reflection and transmission losses at the interfaces. This method was applied for C6_PI (C6_post irradiation), Fig. 4. Uncertainty on R_{dB} obtained in this way may be as high as $\pm$ 3dB which implies that the reflectivity is in an interval [0.1%; 0.4 %].
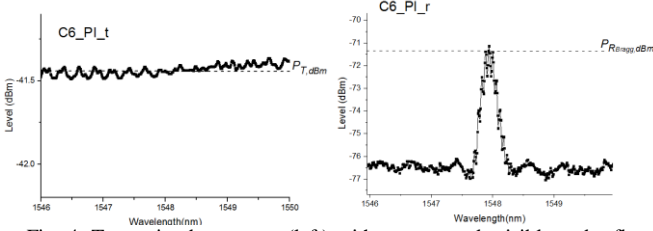

Fig. 4. Transmitted spectrum (left) without any peak visible and reflected spectrum (right) on sample C6_post irradiation, permitting to determine a reflectivity of ~0.2%.

C. Assessment of Bragg Wavelength and BWS.

As far as possible, we determined the Bragg wavelength through a 3rd order polynomial fit on the reflection spectrum with a threshold of 3dB (only wavelengths with a reflection level between the peak and 3dB below were considered for the fit). The maximum of the fit gives the Bragg wavelength. This criterion is labelled as PF (Peak of the Fit criterion).

The accuracy of this or any other criterion may be questioned when the shape of the spectrum changes. See for example reflected spectra of sample A2 in Fig.5.

The BWS obtained with the PF criterion may be compared with the one obtained considering the average of the wavelengths at which the reflection value is 3dB below the peak. We will label this criterion as MB (Mid Band criterion). For the sample A2, with a change in FWHM from 942 pm to 182 pm, the two criteria gave a large BWS with a 13% difference. With Bragg peaks saturated neither before nor after irradiation, then the BWS with both criteria are closer.
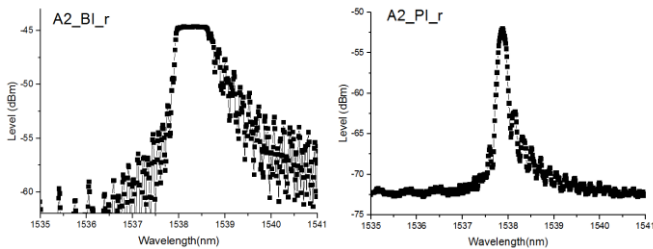

Fig. 5 Reflection spectra of the sample A2 obtained before irradiation (BI, left) and after irradiation (PI, right). The criterion of Peak of the Fit (PF) gives a BWS of -447pm. The criterion of Mid Band (MB) gives a BWS of -513 pm

IV. RESULTS OF FBG CHARACTERIZATION

A. Samples irradiated at fluence $10^{19} n_{fast}/cm^2$

The changes in reflectivity for the samples irradiated up to 10^{19} n_{fast}/cm^2 are presented in Table 5. For saturated FBG, we also indicate the FWHM.

TABLE 5. ATTENUATION OF THE FBG IRRADIATED AT FLUENCE $10^{19} N_{FAST}/CM^2$ (FWHM FOR SATURATED FBG)

FBG	Before Irradiation Reflectivity (FWHM)	Post Irradiation Reflectivity (FWHM)
A1	100% (942 pm)	15%
A2	100% (942 pm)	13%
A3	100% (1114 pm)	20%
B1	100% (1650 pm)	100% (1409pm)
C1	80%	60%
C2	50%	30%
C3	80%	50%
C4	70%	25%
C5	13%	5%

Table 5 shows that samples A1-A3 were severely affected by combined radiation and temperature effects, mainly because they were not thermally annealed after inscription. Nevertheless, the gratings are easily detectable. A decrease of the FWHM could also be noted on the samples C1-C5; for example the bandwidth for C1 changed from 317 pm to 256 pm (data not shown in Table 5).

It appears that the samples with similar characteristics, i.e. A1 and A2, C1 and C3 were affected in the same way. Comparison the loss of reflectivity between C1 to C3 (pre-treated with H_2) and C4 (without H2 loading) tends to show that H_2-loading resulted in a more resistant FBG.

Table 6 reviews the BWS of the samples irradiated at 10^{19} n_{fast}/cm^2. All Bragg wavelengths were extracted through PF criterion on the reflection spectra, except C5 which showed a noisy reflection spectrum after irradiation; then the transmission spectra for both C5_BI and C5_PI measurements were used to determine λ_B.

TABLE 6. SHIFT OF THE FBG IRRADIATED AT FLUENCE $10^{19} N_{FAST}/CM^2$

FBG	λ_B_BI (nm)	λ_B_PI (nm)	BWS (pm)
A1	1538.476	1538.024	- 452
A2	1538.314	1537.867	- 447
A3	1538.879	1538.188	- 691
B1	1538.966	1548.944	- 22
C1	1548.054	1548.043	- 11
C2	1547.964	1547.924	- 40
C3	1548.123	1548.021	- 102
C4	1548.099	1547.962	- 137
C5	1547.991	1547.867	- 124

The MB criterion was also used for sample B1 and C1, giving for B1 +12 pm instead of -22 pm, and for C1 -12 pm instead of -11pm. The temperature of the support was exactly the same during both B1_BI and B1_PI measurements, and the temperature for C1_BI was 0.5 °C larger than for C1_PI, which tends to indicate that the true BWS is rather about 5 pm.

Like for the change of the reflectivity, the samples A1 and A2 having similar initial characteristics exhibit very similar

BWSs. But C1 and C3 samples show quite noticeable difference in BWS (102 pm instead of 11pm); it is even more significant that C1 has a very low BWS. C2 with a lower reflectivity than C1 both before and after irradiation shows also a quite low BWS. Fabricated without H_2-loading, C4 and C5 FBGs seem a bit more affected than FBGs pre-treated with H_2. All the observed BWSs are negative (blue shift).

B. Samples irradiated at $3 \times 10^{19} n_{fast}/cm^2$

We report now the results for samples irradiated in the capsule 2: the neutron fluence was 3 times higher than for capsule 1, as well was the gamma dose (1.5 GGy instead of 0.5 GGy) whereas the gamma and neutron flux and also the temperature of irradiation were identical.

Table 7 reports the changes in reflectivity; for the saturated FBGs, the FWHM is also indicated.

TABLE 7. ATTENUATION OF THE FBG IRRADIATED AT
FLUENCE $3 \times 10^{19} N_{FAST}/CM^2$
(FWHM FOR SATURATED FBG)

FBG	Before Irradiation Reflectivity (FWHM)	Post Irradiation Reflectivity (FWHM)
B2	100% (1960 pm)	100% (1484pm)
C6	5%	0.2%
C7	60%	50%
D1	> 99% (1176 pm)	98% (855pm)
D2	100% (945pm)	100% (1480nm)

We can notice that C7 reflectivity change is ~10%, smaller than that for C4 which had similar reflectivity before irradiation and was irradiated at a lower fluence in capsule 1. The gratings written in the pre-irradiated fibres, D1 and D2 also show changes in the reflection spectrum. Irradiation induced a FHWM decrease on sample D1 (Figure 6) and on the other hand an increase on sample D2; D2 was annealed before irradiation and D1 was not. As a reminder, those samples were difficult to manufacture as no monitoring of the FBG could be done during their writing. Furthermore, the fibre is not SMF28 and has a cut-off wavelength around 900 nm as it was intended for FPSs development with a wavelength bandwidth centred at 970 nm.
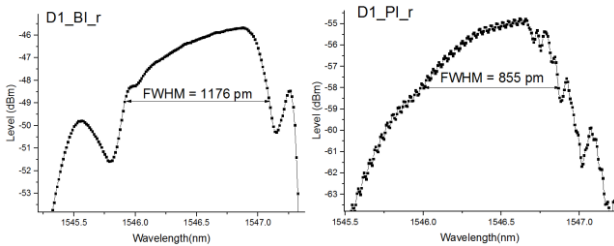

Fig. 6. Spectrum in reflection of the sample D1 obtained before irradiation (BI, left) and after irradiation (PI, right). The FWHM changes from 1176 pm to 855 pm.

Table 8 reviews the BWS of samples irradiated at 3×10^{19} n_{fast}/cm^2. All Bragg wavelengths have been extracted through PF criterion on reflection spectrum. Values obtained through MB criterion are also indicated in brackets.

TABLE 8. SHIFT OF THE FBG IRRADIATED
AT FLUENCE $3 \times 10^{19} N_{FAST}/CM^2$

FBG	λ_{B}_BI (nm)	λ_{B}_PI (nm)	BWS (pm)
B2	1549.054	1548.755	- 299 (-164)
C6	1548.018	1547.933	- 85 (-76)
C7	1547.371	1547.097	- 274 (-300)
D1	1546.697	1546.546	- 151 (-66)
D2	1544.472	1544.260	- 212 (-269)

On samples C6 and C7, with Bragg peaks saturated neither before nor after irradiation, the BWS with both criteria are closer than for B1, D1 and D2.

Others criteria considering the whole shape of the spectrum reflected or transmitted and not only the spectrum 3 dB below the peak have also being tried. A global fit on the transmitted spectrum was used for D2 sample giving a BWS of about -160 pm. Whatever was the selected criterion, the BWS for FBG irradiated at $3 \times 10^{19} n_{fast}/cm^2$ appeared always negative.

V. DISCUSSIONS

The results presented above were obtained for FBGs written in the germanosilicate SMF28 fibre. This fibre is not considered as radiation tolerant as it contains Ge in its core. In spite of that, all FBGs remained visible after irradiation. Results in Table 6 show that type II FBGs written with fs laser @800nm are more radiation resistant than type I FBG written with CW laser as it was already noticed under γ-rays [9, 21].

Not only FBG, but also bare fibre samples were irradiated during the SAKE 2 experiment. Then compaction was measured on SMF28e samples (same fibre as used for FBG sample A1-A3); with similar procedure as described in [7]. The compaction was measured at 0.29% ± 0.05% in capsule 1 and 0.57% in capsule 2. 0.05% corresponds to the maximum error assessment, the standard deviation was less than 0.01% for capsule 1. We also measured the refractive index change with an IFA-100 multi-wavelength Optical Fibre Analyser (measurements made by iXBlue Company, Lannion France). The index change measured was + 0.2% (dn/n= 0.2% +/- 0.02%) for samples in capsule 1.

Let us see which BWS would come out from a calculation relying on the hypothesis that changes inside the FBG can be deduced from changes in the bare material.

Equation (1) gives:

$$\frac{\Delta \lambda_B}{\lambda_B} = \frac{\Delta n_{eff}}{n_{eff}} + \frac{\Delta \Lambda_B}{\Lambda_B} \qquad (5)$$

Assuming that

$$\frac{\Delta n_{eff}}{n_{eff}} = \frac{\Delta n}{n}, \qquad (6)$$

then $\frac{\Delta \lambda_B}{\lambda_B}$ = 0.2 % -0.29%= - 0.09% ± 0.06%, which gives a BWS about -1.4 nm ± 0.9nm (one big value is subtracted from another big value to get a small one; uncertainty is important). While it may not give an accurate result, this simple

calculation shows how structural modification induced by compaction and associated index variation may affect the Bragg wavelength. Largest BWSs obtained in our measurements with FBGs irradiated in capsule1 are about 3 times lower than the average value but still within the error margin. The predicted variation direction agrees with the observation of the negative BWS.

During SAKE 1 we irradiated [7] some gratings similar to samples C, which were not annealed. They were erased after irradiation. That highlights the crucial role of annealing that appears mandatory to enhance the FBG resistance at fast neutrons fluence and high temperatures.

Some FBGs experienced low change in reflectivity and also low BWS: around the equivalent of 1 °C after irradiation in capsule 1 at 10^{19} n_{fast}/cm², and also quite low BWS after irradiation at 3×10^{19} n_{fast}/cm², for C6 the shift is -85pm, which corresponds to - 8.5 °C. We can regret that none such FBG made on H2 loaded fibre was tested since C1-C3, with H_2 loading, seems less sensitive, on the whole, than C4 and C5 in capsule 1.

VI. Conclusion / Perspectives

We have conducted a reactor irradiation of FBGs written in SMF28/ SMF28e fibres from Corning. The samples were exposed to intense mixed neutron-gamma radiation field at two fluences of fast neutrons: 10^{19} and 3×10^{19} n_{fast}/cm². Based on the compaction and refractive index measurements performed on pristine (without FBGs) fibre samples we demonstrated that large observed BWSs could be explained as originating from structural changes, in agreement with the measurements done on the tested standard FBGs.

For some type II FBGs written with a 800 nm fs laser and pre-annealed at a high temperature before neutron exposure, we measured after irradiation quite low change in reflectivity and also low RI-BWS of about 10 pm, equivalent to an associated error of about 1° C for a temperature sensor. Such value remains compatible with the specifications of foreseen temperature measurements in a reactor core.

At the higher level of neutron fluence (3×10^{19} n_{fast}/cm²), the RI-BWSs tend to be larger than at lower fluence (10^{19} n_{fast}/cm²), in agreement with the assessment that the glass compaction has not yet saturated at the lower level.

Tested samples were only few cm long, and even if the irradiated length of future OFS in MTR should only be around 1 m, the use of a rad hard fibre rather than a telecom-grade fibre should be preferred to avoid the negative influence of a too large RIA. FBGs written in rad hard fibres are known to perform well under gamma irradiation, we also tested some in SAKE 2 with indeed some limited reflectivity decrease and the BWS down to less than 10 pm.

The radiation induced changes in the shape of the reflected or transmitted spectrum make the choice of the criterion to extract the Bragg wavelength important. We have reported that in such a case variations of the BWS retrieved when changing the criterion can be significant. That also implies the importance of using gratings with a well-defined Bragg peak to allow maintaining the quality of temperature measurements.

It is useful to remind that SAKE irradiation has been made at 250°C; our measurements of compaction (not reported here in detail) seem to show that the irradiation temperature could have an influence on compaction. As a consequence, we could then expect different RI-BWS at higher temperatures, due to the effects of higher temperature levels on radiation effects on silica glasses.

We also look forward to perform experiments with continuous monitoring for more comprehensive information on how the BWS and reflectivity of rad hard FBGs evolve when exposed to fast neutrons. Such measurements will allow to provide better evidence for the impact of compaction (and its saturation) on the FBG radiation response.

References

[1] G. Bignan, J. F. Villard, C. Destouches, P. Baeten, L. Vermeeren, and S. Michiels, "The key-role of instrumentation for the new generation of research reactors," ANIMMA Int. Conf. 2011, Gent, Belgium.

[2] F. Jadot, F. Baque, J. Ph. Jeannot, G. De Dinechin, J. M. Augem, and J. Sibilo, "ASTRID Sodium cooled Fast Reactor: Program for improving In Service Inspection and Repair," ANIMMA Int. Conf. 2011, Gent, Belgium.

[3] H. A. Abderrahim, P. Beaten, D. De Bruyn, and R. Fernandez, "MYRRHA – A multi-purpose fast spectrum research reactor," Energy Conversion and Management, Volume 63, pp. 4-10, November 2012.

[4] J.M. López-Higuera, Handbook of optical fibre sensing technology, John Wiley & Sons, New York, 2002, pp. 828.

[5] S. Girard, J. Kuhnhenn, A. Gusarov, B. Brichard, M. Van Uffelen, Y. Ouerdane, A. Boukenter, and C. Marcandella, "Radiation Effects on Silica-Based Optical Fibers: Recent Advances and Future Challenges," IEEE Trans. Nucl. Sci., vol.60, no.3, pp. 2015-2036, 2013.

[6] G. Cheymol, A. Gusarov, S. Gaillot, C. Destouches, and N. Caron, "Dimensional Measurements Under High Radiation With Optical Fibre Sensors Based on White Light Interferometry - Report on Irradiation Tests," IEEE Trans. Nucl. Sci., vol.61, no.4, pp. 2075-2081, 2014.

[7] L. Remy, G. Cheymol, A. Gusarov, A. Morana, E. Marin, and S. Girard, "Compaction in optical fibres and fibre Bragg gratings under nuclear reactor high neutron and gamma fluence," IEEE Transactions on nuclear science, Vol. 63, N°4, August 2016.

[8] W. Primak, "Fast neutron induced changes in quartz and vitreous silica," Phys. Rev.B, vol. 110, no.6, pp. 1240-1254, 1958.

[9] A. Gusarov and S. K. Hoeffgen, "Radiation Effects on Fiber Gratings", IEEE Trans. Nucl. Sci., vol. 60, pp. 2037-2053, 2013.

[10] M. Perry, P. Niewczas, and M. Johnston, "Effects of neutron-gamma radiation on fiber Bragg grating sensors: a review," IEEE Sensors, vol. 99, 2012.

[11] A. Morana, S. Girard, E. Marin, C. Marcandella, P. Paillet, J. Périsse, J.-R. Macé, A. Boukenter, M. Cannas, and Y. Ouerdane, "Radiation tolerant fiber Bragg gratings for high temperature monitoring at MGy dose levels," Opt. Lett. 39, 5313-5316, 2014.

[12] A. Morana, S. Girard, E. Marin, J. Périsse, J. S. Genot, J. Kuhnhenn, J. Grelin, L Hutter, G. Mélin, L. Lablonde, T. Robin, B. Cadier, J. R. Macé, A. Boukenter, and Y. Ouerdane, Radiation-Hardened Fiber Bragg Grating Based Sensors for Harsh Environments," IEEE Transactions on Nuclear Science, vol.64 (1), pp. 68 - 73, 2017, (DOI: 10.1109/TNS.2016.2621165)

[13] J. Kuhnhenn, U. Weinand, A. Morana, S. Girard, E. Marin, J. Perisse, J. Genot, J. Grelin, G. Melin, B. Cadier, T. Robin, J. R. Mace, A. Boukenter, and Y. Ouerdane, "Gamma Radiation Tests of Radiation-Hardened Fiber Bragg Grating Based Sensors for Radiation Environments," in IEEE Transactions on Nuclear Science , vol.PP, no.99, in press, 2017.

[14] A. Gusarov, "Long-term exposure of fiber Bragg gratings in the BR1 low-flux nuclear reactor," IEEE Trans. Nucl. Sci., vol. 57, no. 4, pp. 2044–2048, 2010.

[15] T. Kakuta, H. Yamagishi, T. Iwamura, and M. Urakami, "Development of New Nuclear Instrumentation based on Optical Sensing - Irradiation Effects on Fiber Bragg Grating Sensors," in SPIE 14th International Conference on Optical Fibre Sensors (OFS-14), vol. 4185, pp. 816–819, 2000.

[16] K. Fujita, A. Kimura, M. Nakazawa, and H. Takahashi, "Bragg peak shifts of figre Bragg gratings in radiation environment," in SPIE Conf. Fiber Optic Sensor Technology II, vol. 4204, Boston, MA, pp. 184–191, 2000.

[17] R.S.Fielder, D.Klemer, and K.L.Stinson-Bagby, "High neutron fluence survivability testing of advanced Fiber Bragg Grating sensors," AIP Conference Proceedings, vol. 699, n° 1, pp. 650-657, 2004.

[18] S. Girard, C. Marcandella, A. Morana, J. Perisse, D. Di Francesca, P. Paillet, J-R. Macé, A. Boukenter, M. Léon, M. Gaillardin, N. Richard, M. Raine, S. Agnello, M. Cannas and Y. Ouerdane, "Combined High Dose and Temperature Radiation Effects on Multimode Silica-based Optical Fibers," IEEE Transactions on Nuclear Science, vol.60, n°6, pp. 4305 - 4313, 2013.

[19] AREVA-LabHC pending patent, "Procédé de fabrication d'une fibre optique traitée pour capteur de température résistant aux radiations," deposited Dec. 16th 2013, n°13 62691.

[20] G Laffont, R Cotillard and P Ferdinand, "Multiplexed regenerated fiber Bragg gratings for high-temperature measurement," Measurement Science and Technology, Volume 24, Number 9.

[21] A. Morana et al., "Influence of photo-inscription conditions on the radiation-response of fiber Bragg gratings," Opt. Exp., vol. 23, no. 7, pp. 8659–8669, 2015.